THE JOURNAL OF PHYSICAL CHEMISTRY Letters

Letter

pubs.acs.org/JPCL

Pick and Choose the Spectroscopic Method to Calibrate the Local Electric Field inside Proteins

Tapas Haldar, Somnath M. Kashid, Pranab Deb, Sandeep Kesh, and Sayan Bagchi*

Physical and Materials Chemistry Division, CSIR-National Chemical Laboratory, Dr. Homi Bhabha Road, Pune 411008, India

Supporting Information

ABSTRACT: Electrostatic interactions in proteins play a crucial role in determining the structure−function relation in biomolecules. In recent years, fluorescent probes have been extensively employed to interrogate the polarity in biological cavities through dielectric constants or semiempirical polarity scales. A choice of multiple spectroscopic methods, not limited by fluorophores, along with a molecular level description of electrostatics involving solute−solvent interactions, would allow more flexibility to pick and choose the experimental technique to determine the local electrostatics within protein interiors. In this work we report that ultraviolet/visible-absorption, infrared-absorption, or ^{13}C NMR can be used to calibrate the local electric field in both hydrogen bonded and non-hydrogen bonded protein environments. The local electric field at the binding site of a serum protein has been determined using the absorption wavelength as well as the carbonyl stretching frequency of its natural steroid substrate, testosterone. Excellent agreement is observed in the results obtained from two independent spectroscopic techniques.

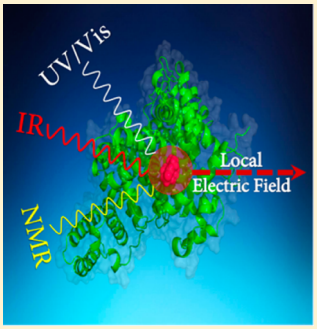

The polarity within protein interiors affects the protein's interactions with ligands, substrates, and other proteins, making it a critical determinant of protein structure, stability, and activity. Because electrostatic interactions are prevalent in any biomolecular system,[1−3] computational and experimental studies have focused on describing local electrostatics and polarity within biological cavities. Protein polarity is often described by a low dielectric constant (ε = 2−4); however, electrostatics calculations suggest large electric fields are produced by charged and polar groups in folded proteins that can vary from site to site in magnitude and direction.[4−6] Experimental studies for protein polarity determination have mostly relied on the sensitivity of the fluorescent probes to the microenvironment.[7,8] These studies are informative and report on protein polarity by correlating peak emission wavelength to dielectric constant or semiempirical solvent polarity parameters and scales.[9−12] However, there are a few limitations: (a) Polarity measurement in protein depends on efficient fluorophore insertion, thus limited by the affinity of the ligand binding site. (b) The fluorescent probe might alter the molecular architecture of the native protein and thereby change the function and stability. (c) The dielectric constant is a bulk solvent property and cannot define the local microenvironment around the optical probe. (d) Most of the semiempirical polarity parameters [with a few exceptions, e.g., $E_T(30)$] cannot account for the specific intramolecular and intermolecular interactions like hydrogen bonding. We therefore require a noninvasive label-free spectroscopic method that probes chemical groups preferably either present in the native proteins or in their natural substrates. We would also require a microscopic and quantitative descriptor of electrostatic interactions inside proteins that is dependent on the molecular architecture of the biomolecule and the coordinates of the surrounding solvent molecules. Moreover, a direct coupling, understood on a theoretical basis and independently verified by experiments, should exist between the spectroscopic observable and the local electrostatics descriptor.

Carbonyl (C═O) groups are ubiquitous in biomolecules and are also common in the natural substrates of the proteins. Probing C═O moieties paves the way to use label free spectroscopic techniques. Here, we focus on noninvasive spectroscopic methods like infrared (IR) spectroscopy, nuclear magnetic resonance (NMR) spectroscopy, and ultraviolet/visible (UV/vis) n−π^* absorption spectroscopy that provide spectral signatures of the C═O moiety. Moreover, the spectroscopic observables like C═O IR frequencies, ^{13}C NMR chemical shifts of the C═O carbon, or n−π^* wavelengths are sensitive to the immediate surroundings of the C═O group and therefore should be ideal to report on the local electrostatics within proteins.[13−16] The electric field estimated at any point inside the protein depends on the distances of all the other atoms in the system (both solute and solvent atoms) from that point as well as the residual partial charges on each atom and has been reported to influence every aspect of protein function.[17,18] Because biomolecules consist of polar, polarizable, and charged residues, the electric field experienced by C═O from its environment can provide microscopic insight about how enzymes function within the highly heterogeneous protein environment.[14] For example, a small change in the environment, such as a modification in the protonation state or a conformational rearrangement upon

Received: April 20, 2016
Accepted: June 13, 2016
Published: June 13, 2016

DOI: 10.1021/acs.jpclett.6b00852
J. Phys. Chem. Lett. 2016, 7, 2456−2460

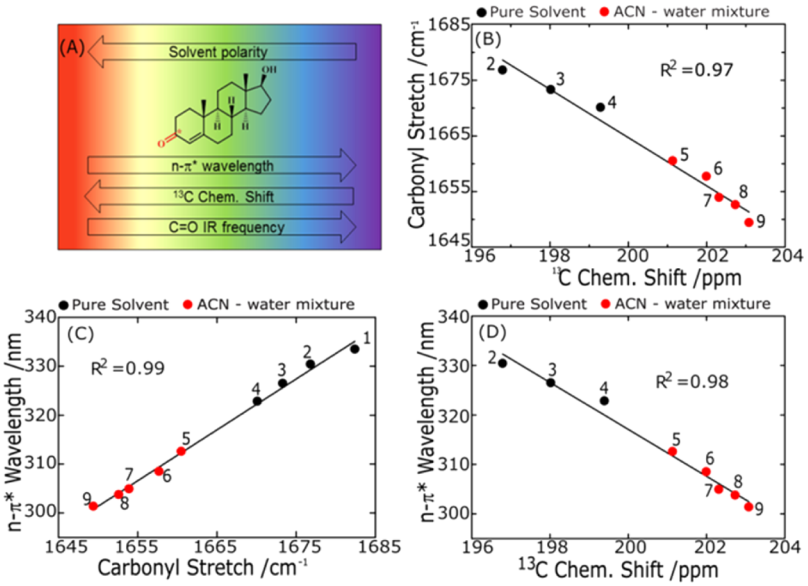

Figure 1. For carbonyls, the spectroscopic observables of IR spectroscopy, NMR spectroscopy, and UV/vis absorption spectroscopy change with the solvent polarity. Panel A represents the shift (and the direction of the shifts) in the observables for testosterone with the varying solvent polarity. Linear correlations exist among the three independent spectroscopic observables of testosterone, namely, (B) C═O stretching frequency and ^{13}C chemical shift of the C═O carbon, (C) C═O stretching frequency and n−π* wavelength, and (D) n−π* wavelength and ^{13}C chemical shift of the C═O carbon in hydrogen bonding and non-hydrogen bonding solvents. The black lines denote the best-fit lines; the black circles represent aprotic solvents [(1) DBE, (2) THF, (3) VLN, (4) ACN], and red circles represent protic binary solvent mixtures [(5) A10W, (6) A20W, (7) A30W, (8) A40W, (9) A50W]. The regression values of the fitted lines are shown in the figures.

ligand binding, would result in a change in the electric field experienced by C═O. Moreover, because C═O hydrogen bonding interactions are electrostatic,[15,19] the electric field at C═O includes specific solute−solvent interactions like hydrogen bonding. In this work, we have shown independent linear correlations of IR, NMR, and UV/vis spectroscopic observables to the electric field exerted on C═O. Depending on the biomolecular system, we can pick and choose the spectroscopic method to determine the local electric field within biomolecules.

Serum albumins, one of the most abundant proteins in the circulatory system, maintain osmotic pressure and pH of blood and transport several lipophilic compounds, such as fatty acids, drugs, and steroid hormones. Testosterone, a steroid hormone, is one of the natural substrates of serum albumins. The association of testosterone with serum proteins regulates its biological activity. The steroid−protein interaction has major biological implications, and the local electric field at the testosterone binding site of bovine serum albumin (BSA) has been probed in the present work.

To interrogate the local electrostatics at the binding site of BSA, solvatochromic IR, ^{13}C NMR, and UV/vis experiments were performed for testosterone in a wide range of solvation environments of varying polarity. Testosterone was dissolved in various organic solvents and binary aqueous mixtures of acetonitrile/water to mimic non-hydrogen bonding and hydrogen bonding solvation environments of the substrate. Due to the change in polarity, a shift in the respective peak positions is observed in each of the spectroscopic techniques (Figure 1A). The n−π* absorption wavelength of testosterone shows a monotonically increasing blue-shift with the increasing polarity of the aprotic solvents and the protic aqueous binary mixtures (with increasing water content) (Table 1). The C═O stretching frequency of testosterone shows a monotonic red shift with the increasing polarity of the same set of neat solvents

Table 1. n−π* Absorption Wavelength, C═O Stretching Frequencies, and ^{13}C NMR Chemical Shifts for Testosterone in Non-hydrogen Bonding and Hydrogen Bonding Solvents

serial no.	solvent	n−π* wavelength (nm)	carbonyl stretch (cm^{-1})	^{13}C chemical shift (ppm)
1	dibutyl ether (DBE)	333.47	1682.4	No peak
2	tetrahydrofuran (THF)	330.39	1676.8	196.79
3	valeronitrile (VLN)	326.50	1673.3	198.02
4	acetonitrile (ACN)	322.80	1670.1	199.39
5	90% ACN + 10% water (A10w)	312.57	1660.5	201.39
6	80% ACN + 20% water (A20W)	308.50	1657.7	201.99
7	70% ACN + 30% water (A30W)	304.93	1653.9	202.31
8	60% ACN + 40% water (A40W)	303.77	1652.6	202.73
9	50% ACN + 50% water (A50W)	301.37	1649.4	203.08

and solvent mixtures (Table 1). The ^{13}C NMR chemical shift of the carbonyl carbon shows a downfield shift with the increasing polarity of the solvation environment (Table 1). We observe linear cross correlations within the spectroscopic observables in various non-hydrogen bonded as well as hydrogen bonded environments (Figure 1B−D). This result illustrates that measurement of one of the spectroscopic observables can directly predict the other observables from the calibrations shown in Figure 1. To verify the generality of the linear correlation between independent spectroscopic variables as seen for testosterone C═O, we have performed solvatochromic experiments on small molecule ketones, esters, and amides, and the results show trends similar to those found in testosterone (shown in the Supporting Information). Thus, a

DOI: 10.1021/acs.jpclett.6b00852
J. Phys. Chem. Lett. 2016, 7, 2456−2460

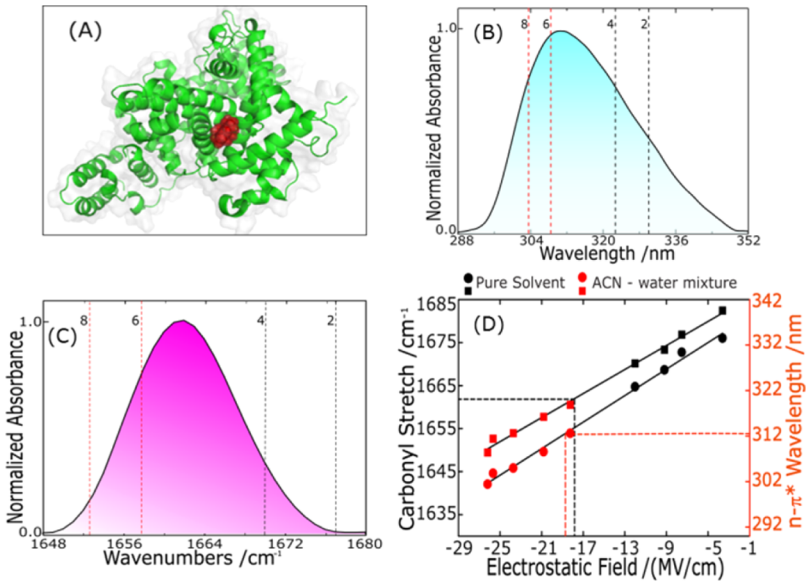

Figure 2. (A) Cartoon of BSA−testosterone complex. The protein is shown in green, and the substrate is shown in red. (B) The n−π^* absorption spectra and (C) the IR spectra of C═O stretch of testosterone in BSA−testosterone complex can be used to estimate the local polarity at the binding site of BSA using electric field (D). The predicted electric fields from UV/vis and IR experiments are within 0.7 MV/cm (error ∼3.5%). The dotted vertical lines in panels B and C represent the peak maxima of aprotic solvents and binary aqueous mixtures. The numbers (2, 4, 6, and 8) correspond to those in column 1 of Table 1.

direct coupling of any of these spectroscopic variables to the local electric field within the biomolecular interior would allow us to quantify local electrostatics by performing any one of the above-mentioned noninvasive spectroscopic experiments.

Interestingly, the C═O IR frequencies are known to show linear sensitivity toward the electrostatic field through vibrational Stark effect (VSE).[20] A change in the local environment modifies the electrostatic field exerted on the IR probe, thereby causing a shift in the IR transition energy. Moreover, vibrational Stark tuning rate, the change in IR frequency caused by a unit change in field, can be measured independently from vibrational Stark spectroscopy (VSS). For a diatomic chemical moiety like C═O, the varying electrostatic field along the C═O bond in solvatochromic experiments polarizes the charge density and changes the perpendicular elements of the shielding tensor.[21] The change in charge density changes the shielding on the C═O carbon nucleus, and the ^{13}C chemical shift has been reported to vary linearly with the field. Thus, while the linear sensitivity of C═O to electrostatic field is the difference dipole (VSE) that for ^{13}C NMR is the shielding polarizability. Because both C═O stretching frequencies and ^{13}C chemical shifts of the C═O carbon show linear sensitivity toward electrostatic field, the electrical and magnetic properties of the ground electronic state tend to vary linearly (Figure 1B). The linear correlation between C═O IR frequencies and the n−π^* absorption wavelengths arises as the solvent shell orientation in the Franck−Condon state is adapted to the electrostatic interactions of the ground state. The excitation process is much faster than the solvent shell reorientation process, and the solvatochromic shifts of the n−π^* transitions are dominated by the ground-state electrostatic stabilization of the spectroscopic probe.[22]

The tuning rate of 19-nortestosterone (another steroid with a similar structure) has been measured and reported by Boxer and co-workers.[14] Using molecular dynamics (MD) simulations, we have calculated the electrostatic field at the midpoint of the C═O of testosterone in all the different solvation environments of the solvatochromic experiments. The calculated fields, corrected using the experimentally measured Stark tuning rate (see Supporting Information for details) show a linear correlation with the C═O IR frequencies (Figure 2). ^{13}C NMR chemical shifts of the C═O carbon and the n−π^* absorption wavelengths also show similar linear sensitivities to the calculated electrostatic fields as expected from Figure 1. The straight lines shown in Figure 2D can independently calibrate the sensitivities of C═O IR frequency, ^{13}C chemical shift (shown in Figure S15 of the Supporting Information), and n−π^* wavelength to the electrostatic field exerted on the carbonyl at the testosterone binding site of the serum protein.

The binding constant (K_a) of 8.89 (±1) × 10^4 M^{-1} is obtained for BSA-testosterone complex using tryptophan fluorescence quenching of the protein. This result shows good agreement with the previously reported value of K_a by Tajmir-Riahi and co-workers.[23] For the spectroscopic experiments of the protein−steroid complex, 1 mM of testosterone was added to 1.5 mM BSA solution in phosphate buffer (pH 7.0). At these concentrations, >99% of the steroid is bound to the serum protein, implying that the detected spectroscopic signals of the ligand reflect that of the bound state. The n−π^* absorption wavelength and the C═O stretching frequency of testosterone observed in 1:1 BSA-testosterone complex are 312.6 nm (Figure 2A) and 1661.7 cm^{-1} (Figure 2B), respectively. It is important to note that the experimentally observed C═O IR frequency shows excellent agreement with the frequency predicted from the n−π^* wavelength, 1660.8 cm^{-1}, by the calibration curve in Figure 1B. The corresponding electrostatic fields predicted from the peak maxima of the n−π^* absorption spectrum and the C═O IR spectrum at the BSA binding site of testosterone are −18.70 and −18.03 MV/cm (Figure 2C), respectively. A negligible ∼3.5% error in the field estimation from the independent spectroscopic techniques illustrates that either of these noninvasive experimental methods can be used to predict the local electric field at the binding site of the protein.

DOI: 10.1021/acs.jpclett.6b00852
J. Phys. Chem. Lett. 2016, 7, 2456−2460

Apparently, testosterone senses a large electric field at the binding site of BSA that is similar to that sensed by testosterone in a polar (10% acetonitrile/water) solvent. The electric fields in solution are homogeneous and increase with the overall solvent polarity. However, a nominally nonpolar protein matrix with surface charges can produce an inhomogeneous electric field similar to that in polar solvation environment required for the spectroscopic shift. In a recent work by Boxer and co-workers, an extremely large electric field was found to be exerted on the substrate by the oxyanion hole at the active site of an enzyme.[14] Semiempirical polarity parameters provide only a qualitative understanding and fail to depict a microscopic description of the structure−function relation. The electrostatic field on the other hand serves as a quantitative and microscopic descriptor of local electrostatics and can be estimated from multiple choices of spectroscopic experiments as well as molecular dynamics (MD) simulations.

The implications of these results are manifold. We have shown that IR, UV/vis, or ^{13}C NMR experimental techniques can be used to calibrate the local electric field within protein interiors. Choice of the spectroscopic technique depends on the concerned biological/chemical process. For example, n−π^* absorption might be the favored technique to determine electric field for protein−ligand complexes where the absorption peak of the ligand can be monitored, as shown in this work. A long wavelength n−π^* absorption of the ligand (as seen in testosterone) has less overlap with the protein absorption as compared with the overlap of the carbonyl stretch with the amide I protein IR band. Another inherent technical advantage of UV/vis spectroscopy over IR spectroscopy in the case of protein ligand complexes arises from the ease of subtracting the background protein spectra. The commonly used IR sandwich sample cells make it difficult to maintain the same path length in individual IR measurements. However, no such error from the reproducibility of the path length arises for the standard cuvettes (fixed path length) used for UV/vis absorption experiments. On the other hand, isotope editing ($^{13}C{=}O$ or $^{13}C{=}^{18}O$) has been extensively used to isolate the C═O frequencies of a specific amino acid in a protein. In such cases, both IR as well as ^{13}C NMR will be able to provide the local electric field within the protein interior. However, the electric field should be projected along the direction of the transition dipole of the amide normal mode which is not along the C═O bond as shown here for testosterone. These results are also significant from the computational viewpoint. When crystal structures are unavailable for protein−substrate complexes, molecular docking provides a snapshot of the orientation of the substrate with the biomolecule. However, multiple orientations of the ligand with respect to the receptor might be equally probable as predicted from docking studies. MD simulations of each of these conformers and subsequent electric field estimation when compared with the electric field predicted from the spectroscopic experiments can underpin the orientation of the substrate at the binding site and provide a molecular level picture of the biological process.

EXPERIMENTAL SECTION

Testosterone; bovine serum albumin; and solvents, such as dibutyl ether, tetrahydrofuran, valeronitrile, acetonitrile, and D_2O, were obtained from Sigma-Aldrich and used without further purification. UV absorption spectra were measured on a Shimadzu UV 3600 Plus spectrophotometer using a quartz cell of 1 cm path length. The concentration of testosterone used for solvatochromic UV/vis absorption experiments was 5 mM. The ^{13}C NMR spectra were obtained on a 400 MHz JEOL ECX NMR spectrometer. Here, peak positions were reported as the maximum value. IR absorption spectra were recorded on a FTIR-8300 (Shimadzu) spectrometer with 2 cm^{-1} resolution at room temperature. For each sample (testosterone), ∼60 μL of the sample solution was loaded into a demountable cell consisting of two windows (CaF_2, 3 mm thickness, Shenzen Laser), separated by a mylar spacer of 56 μm thickness. Testosterone was dissolved independently in aprotic solvents and protic binary aqueous mixtures (acetonitrile/water) such that the final concentration of liquid sample is 10 mM for the solvatochromic IR studies. More details about the IR spectroscopy are given in the Supporting Information. The details of the MD simulations and electric field calculations are given in the Supporting Information.

ASSOCIATED CONTENT

Supporting Information

The Supporting Information is available free of charge on the ACS Publications website at DOI: 10.1021/acs.jpclett.6b00852.

Experimental methods and simulation protocol, spectroscopic correlations for other carbonyls, binding constant determination, and table for dielectric constants in various acetonitrile/water mixtures (PDF)

AUTHOR INFORMATION

Corresponding Author

*E-mail: s.bagchi@ncl.res.in.

Notes

The authors declare no competing financial interest.

ACKNOWLEDGMENTS

This work was financially supported by CSIR-NCL (Grant MLP028126) and SERB, India (SR/S2/RJN-142/2012). Dr. Santosh Kumar Jha (CSIR-NCL) and Dr. Partha Hazra (IISER-Pune) are acknowledged for helpful discussions. P.D. thanks DST for INSPIRE fellowship.

REFERENCES

(1) Warshel, A. Electrostatic Basis of Structure-Function Correlation in Proteins. *Acc. Chem. Res.* **1981**, *14*, 284−290.
(2) Perutz, M. Electrostatic Effects in Proteins. *Science* **1978**, *201*, 1187−1191.
(3) Sharp, K. A.; Honig, B. Electrostatic Interactions in Macromolecules: Theory and Applications. *Annu. Rev. Biophys. Biophys. Chem.* **1990**, *19*, 301−332.
(4) Honig, B.; Nicholls, A. Classical Electrostatics in Biology and Chemistry. *Science* **1995**, *268*, 1144−1149.
(5) Simonson, T. Macromolecular Electrostatics: Continuum Models and Their Growing Pains. *Curr. Opin. Struct. Biol.* **2001**, *11*, 243−252.
(6) Warshel, A.; Papazyan, A. Electrostatic Effects in Macromolecules: Fundamental Concepts and Practical Modeling. *Curr. Opin. Struct. Biol.* **1998**, *8*, 211−217.
(7) Macgregor, R. B.; Weber, G. Estimation of the Polarity of the Protein Interior by Optical Spectroscopy. *Nature* **1986**, *319*, 70−73.
(8) Zhuang, Y.-D.; Chiang, P.-Y.; Wang, C.-W.; Tan, K.-T. Environment-Sensitive Fluorescent Turn-On Probes Targeting Hydrophobic Ligand-Binding Domains for Selective Protein Detection. *Angew. Chem., Int. Ed.* **2013**, *52*, 8124−8128.
(9) Reichardt, C. Solvatochromic Dyes as Solvent Polarity Indicators. *Chem. Rev.* **1994**, *94*, 2319−2358.

DOI: 10.1021/acs.jpclett.6b00852
J. Phys. Chem. Lett. 2016, 7, 2456−2460

(10) Grunwald, E.; Winstein, S. The Correlation of Solvolysis Rates. *J. Am. Chem. Soc.* **1948**, *70*, 846−854.
(11) Kosower, E. M. The Effect of Solvent on Spectra. I. A New Empirical Measure of Solvent Polarity: Z-Values. *J. Am. Chem. Soc.* **1958**, *80*, 3253−3260.
(12) Langhals, H. Polarity of Binary Liquid Mixtures. *Angew. Chem., Int. Ed. Engl.* **1982**, *21*, 724−733.
(13) de Dios, A.; Pearson, J.; Oldfield, E. Secondary and Tertiary Structural Effects on Protein NMR Chemical Shifts: An ab Initio Approach. *Science* **1993**, *260*, 1491−1496.
(14) Fried, S. D.; Bagchi, S.; Boxer, S. G. Extreme Electric Fields Power Catalysis in the Active Site of Ketosteroid Isomerase. *Science* **2014**, *346*, 1510−1514.
(15) Fried, S. D.; Bagchi, S.; Boxer, S. G. Measuring Electrostatic Fields in Both Hydrogen-Bonding and Non-Hydrogen-Bonding Environments Using Carbonyl Vibrational Probes. *J. Am. Chem. Soc.* **2013**, *135*, 11181−11192.
(16) Renge, I. Solvent Dependence of n−π^* Absorption in Acetone. *J. Phys. Chem. A* **2009**, *113*, 10678−10686.
(17) Fried, S. D.; Boxer, S. G. Measuring Electric Fields and Noncovalent Interactions Using the Vibrational Stark Effect. *Acc. Chem. Res.* **2015**, *48*, 998−1006.
(18) Deb, P.; Haldar, T.; Kashid, S. M.; Banerjee, S.; Chakrabarty, S.; Bagchi, S. Correlating Nitrile IR Frequencies to Local Electrostatics Quantifies Noncovalent Interactions of Peptides and Proteins. *J. Phys. Chem. B* **2016**, *120*, 4034−4046.
(19) Kashid, S. M.; Bagchi, S. Experimental Determination of the Electrostatic Nature of Carbonyl Hydrogen-Bonding Interactions Using IR-NMR Correlations. *J. Phys. Chem. Lett.* **2014**, *5*, 3211−3215.
(20) Boxer, S. G. Stark Realities. *J. Phys. Chem. B* **2009**, *113*, 2972−2983.
(21) Augspurger, J. D.; Dykstra, C. E.; Oldfield, E. Correlation of Carbon-13 and Oxygen-17 Chemical Shifts and the Vibrational Frequency of Electrically Perturbed Carbon Monoxide: a Possible Model for Distal Ligand Effects in Carbonmonoxyheme Proteins. *J. Am. Chem. Soc.* **1991**, *113*, 2447−2451.
(22) Haldar, T.; Bagchi, S. Electrostatic Interactions Are Key to C═O n-π^* Shifts: An Experimental Proof. *J. Phys. Chem. Lett.* **2016**, *7*, 2270−2275.
(23) Chanphai, P.; Vesper, A. R.; Bekale, L.; Berube, G.; Tajmir-Riahi, H. A. Transporting Testosterone and its Dimers by Serum Proteins. *J. Photochem. Photobiol., B* **2015**, *153*, 173−183.

DOI: 10.1021/acs.jpclett.6b00852
J. Phys. Chem. Lett. 2016, 7, 2456−2460